MATERIALS PHYSICS AND MECHANICS RESEARCH ARTICLE

Submitted: November 23, 2025 **Revised: February 3, 2026** **Accepted: February 16, 2026**

Parameter identification of the Norton-Bailey creep model using isochronous curves

R.V. Fedorenko ✉, **A.V. Lukin**

Peter the Great State Polytechnical University, St. Petersburg, Russia

✉ fedorenko_rv@spbstu.ru

ABSTRACT

Structural integrity assessment of metal components in advanced reactor systems operating at elevated temperatures requires calculations that account for the sequence and duration of loading throughout their service life. Numerical simulation of such processes is performed using nonlinear inelastic material models, whose parameters are determined based on experimental data. The development and verification of an automated numerical algorithm for identifying the parameters of the Norton-Bailey creep law are considered. The algorithm utilizes initial data in the form of a set of material isochronous curves at a specific temperature. It implements an optimization procedure aimed at minimizing the discrepancy between the normative and the computed isochronous curves. The generation of the computed isochronous curves is performed using the Abaqus software package. It is demonstrated that the developed algorithm enables the highly accurate identification of the constants for the Norton-Bailey law.

KEYWORDS

creep • parameter identification • isochronous curves • optimization • closed nuclear fuel cycle

Funding. *The research is partially funded by the Ministry of Science and Higher Education of the Russian Federation as part of the World-class Research Center program: Advanced Digital Technologies (contract No. 075-15-2022-311 dated 20.04.2022).*

Citation: Fedorenko RV, Lukin AV. Parameter identification of the Norton-Bailey creep model using isochronous curves. *Materials Physics and Mechanics*. 2026;54(1): 118–129.
http://dx.doi.org/10.18149/MPM.5412026_11

Introduction

Currently, nuclear power plants are one of the primary sources of energy generation. A major challenge associated with nuclear power is the depletion of natural resources for fuel production. Consequently, extensive global efforts are underway to reduce their consumption and seek alternative energy sources. Within the framework of the concept for achieving technological leadership of the Russian Federation, the necessity of developing highly efficient energy systems has been outlined. This includes the development of closed nuclear fuel cycle technology and the creation of a thermonuclear reactor capable of producing more energy than it consumes to initiate the fusion reaction [1]. To achieve these goals, development is currently ongoing on fast-neutron reactors with liquid metal coolant and the domestic TRT thermonuclear reactor [2–4]. A key operational feature of such facilities is high temperatures, for instance, exceeding 450 °C during normal operation and up to 900 °C in accident scenarios for the fast-neutron reactors. Designing structures for such temperatures is complicated by the occurrence of significant thermal deformations in the system and the necessity to account for the long-term properties of materials.

Publisher: Peter the Great St. Petersburg Polytechnic University

"The theory of plasticity was brought to life primarily by the needs of turbine construction; subsequently, it found application in nuclear power, chemical engineering, aviation, and rocket technology" is a quote from the fundamental work of Yu.N. Rabotnov, "Creep of Structural Elements" [5]. Indeed, 60 years after the publication of this work, the relevance of creep issues as applied to critical structural components remains undiminished.

Material creep under high temperatures and significant load durations can pose challenges in strength substantiation. In addition to the reduction in the general strength characteristics of the material, issues such as long-term cyclic strength [6] and structural stability under creep conditions arise [7,8].

Regulatory approaches to the strength substantiation of reactor installations [9,10] prescribe simplified procedures within elastic formulations. For instance, accounting for long-term material characteristics at elevated temperatures involves reducing allowable stresses according to the material's isochronous curves; however, this approach possesses significant conservatism. In practice, it is quite difficult to meet the criteria for long-term static and long-term cyclic strength for structural components operating at elevated temperatures within elastic formulations.

Nuclear industry standards [9,10] allow for the possibility of performing strength calculations that consider nonlinear material properties (hardening, creep, microstructure, etc.). In the realm of creep theory, a wide variety of different models exists, each with certain advantages and disadvantages.

Deformation of a material by the creep mechanism is traditionally divided into 3 stages [5]. The first stage is interesting from the perspective of material behavior and the mechanisms of creep initiation, where strain increases non-uniformly over time, eventually reaching a constant rate, which marks the beginning of the second creep stage. During the second (steady-state) stage creep strains accumulate linearly with time. The third stage shows a rapid increase in strain, typically associated with the onset of material failure (hence, engineers often do not consider this zone).

Two basic models are commonly used to describe secondary creep:

1. Power law (the Norton model [11]): $\dot{\varepsilon} = A\sigma^n$, where A and n are material parameters. The advantage of this law is its simplicity, but this is also its drawback: integrating the relation shows that ε depends linearly on time, which hinders the description of a family of isochronous curves with a single set of parameters.
2. Modified power law (the Norton-Bailey model [12]): $\dot{\varepsilon} = A\sigma^n t^m$, where m is a material parameter. This model is the most widespread in engineering practice due to its simplicity from the standpoint of parameter identification [13]. It is free from the drawback of the basic Norton model regarding linear time dependence.

To additionally account for the primary creep stage, one can use, for example, the Darveaux model [14]. In this model, the secondary stage is described by a relation that does not include a time component and can be used independently to describe secondary creep using the hyperbolic sine law $\dot{\varepsilon}_s^{cr} = C_{ss}[\sinh(\alpha\tilde{q})]^n e^{\left(-\frac{Q}{R(\theta-\theta^Z)}\right)}$, where C_{ss} and α are material constants, Q is the activation energy, R is the universal gas constant, θ is the temperature, θ^Z is the absolute zero temperature in the adopted system of units.

Accounting for the non-steady-state component allows for describing the progression of primary creep: $\dot{\varepsilon}^{cr} = \dot{\varepsilon}_s^{cr}\left[1 + \epsilon_T B e^{(-B\dot{\varepsilon}_s^{cr} t)}\right]$, where ϵ_T and B are material parameters.

For describing tertiary creep, models enhanced with material damage parameters can be used, for example, according to the Kachanov-Rabotnov model [15–19]. Based on it, various models considering material damage can be formulated [20,21]. For instance, the Othman model [22]: $\dot{\varepsilon} = \frac{A}{(1-\omega_1)(1-\omega_2)^n}\sinh(B\sigma)$, $\dot{\omega}_1 = C(1-\omega_1)^2\dot{\varepsilon}$, $\omega_1 = 1 - \frac{\rho_1}{\rho}$, $\dot{\omega}_2 = \frac{\dot{\varepsilon}}{3\varepsilon_u}\left(\frac{\sigma_1}{\sigma_e}\right)^v$, where ω_1 and ω_2 are two damage parameters. ω_1 accounts for the role of increasing dislocation density ρ during creep, ω_2 represents damage due to void formation in the material (cavitation), ρ_1 is the initial dislocation density, σ_1 is the first principal stress, σ_e is the effective stress, and $A,\ B,\ C,\ n,\ v,\ \varepsilon_u$ are material constants.

Due to the lack of a unified model, it is often challenging in practice to identify parameters for a specific material model that is most suitable for a given problem. Necessary data for commonly used materials can often be found, but in most cases, difficulties may arise in searching for parameters. For example, standard [23] presents isochronous curves for most structural steels, and standard [9] provides parameters for a specific creep model for some of them. For certain classes of materials, work has been done to identify parameters for various creep models. In [13], parameter identification for the Norton-Bailey model is performed using a regression approach. The procedure for identifying parameters for modeling tertiary creep using the Nelder-Mead method for VZhM4 and VZhM5U alloys is described in [24]. In [25], the selection of creep and plasticity parameters for ZhS32 alloy at elevated temperatures is carried out. In [26], based on an experiment with multi-step loading of a specimen under creep conditions, parameters for the Liu-Murakami [27] damage-based model (for describing all creep stages) are fitted. The results of identification procedure using Levenberg-Marquardt algorithm for unified models describing steady-state and transient creep in [28]. In [29], a two-layer algorithm is proposed for the rapid identification of parameters in a fractional-order creep model of piezoelectric actuator.

The aim of the present research is to develop an automated algorithm for identifying creep parameters, using a family of isochronous curves at a specific temperature as the initial data. At the first stage of development, parameter identification for the modified Norton-Bailey model [12] is performed, as this model is widely used in engineering practice.

Method

The parameter identification procedure is conducted in two stages. The first stage involves the direct identification of the model parameters based on a set of isochronous curves. The second stage entails the numerical solution of a verification problem: uniaxial tension of a specimen, considering the implemented creep model and the identified parameters, using the Abaqus software [30]. The results are then compared with the original isochronous curves. The choice of Abaqus for verification is justified by its convenience for implementing user-defined creep models, its accuracy in solving nonlinear problems, and its recognition by the scientific community as a research tool.

The simplest model from the parameter identification standpoint is the time-hardening form of the Norton-Bailey law [12]:

$$\dot{\varepsilon}_{cr} = \varepsilon_0 \left(\frac{\tilde{q}}{\sigma_0}\right)^n (\varepsilon_0 t)^m, \quad (1)$$

where $\varepsilon_0, \sigma_0, n, m$ are the identifiable model parameters, $\dot{\varepsilon}_{cr}$ is the creep strain rate, t is the time, and $\tilde{q}$ is the equivalent stress.

It is worth noting that the Russian standard GOST [9] recommends a truncated form of this model (without the time component) for accounting for creep in nonlinear strength calculations. A universal reference with parameters for this model for an arbitrary material, across various durations and temperatures, does not exist. In Abaqus [30], it is possible to specify separate parameter values for different temperatures; therefore, identification is performed separately for each temperature, therefore, the identifiable parameters become temperature-dependent, although in the classical approach, only parameters ε_0 and σ_0 exhibit temperature dependence according to the Arrhenius equation. The procedure's workflow is conveniently demonstrated using a real material example. We consider structural steel 12Kh18N12T/12Kh18N10T (AISI 321), used for some critical components of reactor installations. GOST [9] provides isochronous curves for this material; for demonstration, the curves at a temperature of 550°C are considered (Fig. 1).

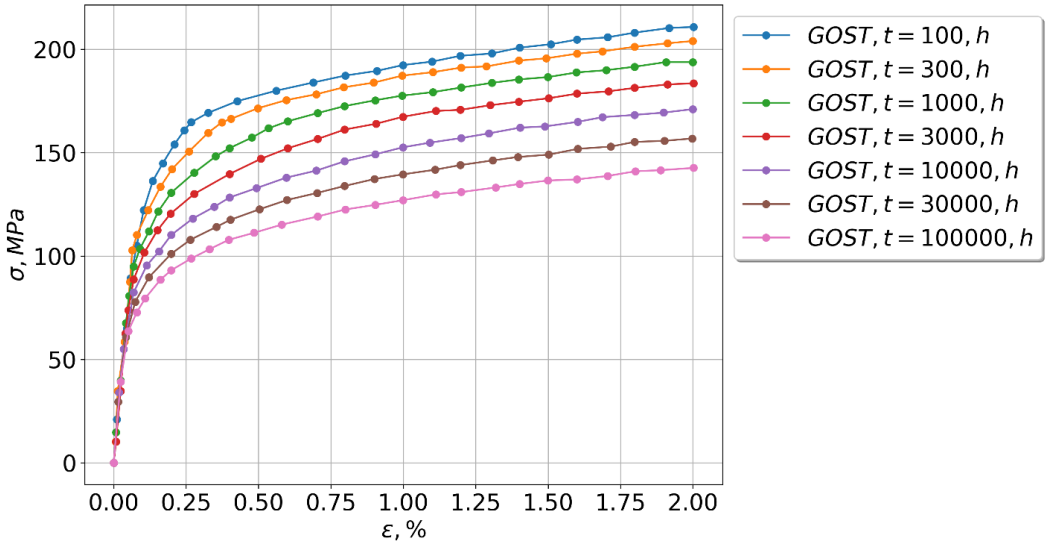

Fig. 1. Isochronous curves for 12Kh18N12T/12Kh18N10T (AISI 321) steel, T = 550 °C

During parameter identification, it is assumed that the loading rate in the experimental studies was constant, with the time for the corresponding isochronous curve taken at 2 % strain ($\varepsilon = 0.02$). Then, taking the experimental time denoted on the standard curves as τ, the following holds:

$$\dot{\varepsilon}_{cr} = \frac{0.02}{\tau}. \quad (2)$$

Consequently,

$$\varepsilon_0^{m+1} \left(\frac{\tilde{q}}{\sigma_0}\right)^n t^m = \frac{0.02}{\tau}. \quad (3)$$

To facilitate algorithm development, a transition is made to a direct dependence of stress on strain:

$$\tilde{q} = \sigma_0 \left[\frac{0.02}{\tau}\ \varepsilon_0^{-m-1} \cdot t^{-m}\right]^{1/n}. \tag{4}$$

The goal of the procedure is to find parameters in the last relation that ensure coincidence with the original isochronous curves for all considered times. The parameter search uses a global minimum search procedure based on the simplicial homology global optimization (SHGO) method [31]. Briefly, the algorithm uses concepts from combinatorial integral homology theory to find subdomains that are approximately locally convex and characterizes the objective function as it runs. It solves a derivative-free optimization problem with constraints (CDFO) [32,33] of the form:

$$\begin{aligned} &\min f(x), \quad x \in \mathbb{R}^n. \\ &g_i(x) \geq 0, \ \forall i = 1, \dots, m, \\ &h_j(x) = 0, \ \forall j = 1, \dots, p, \end{aligned} \tag{5}$$

where x is the vector of variables/parameters, $f(x)$ is the objective function ($f: \mathbb{R}^n \to \mathbb{R}$), $g_i(x)$ are inequality constraints, $h_j(x)$ are equality constraints, and $x_l \leq x \leq x_u$ are the lower and upper bounds for the parameters.

The functional is constructed individually for each problem. Since the research aim is to find a single set of parameters describing the family of isochronous curves, a functional combining several sub-functionals of the same order is adopted:

$$F = \sum_{i=1}^{nfs} f_i \to min, \tag{6}$$

where index $nfs = 5$ indicates the number of sub-functionals to be described below. This allows for the simultaneous control of several criterion values reflecting different characteristics of the compared isochronous curves.

Sub-functional f_1 is the classical Frobenius norm [34]:

$$f_1 = \frac{||Y - X||}{||X||}, \tag{7}$$

where X is the matrix of values for the approximating curves, and Y is the matrix of values for the approximated curves.

In the procedure, all curves (approximating and approximated) are interpolated onto the same grid of abscissa values (strains of the isochronous curves). Thus, matrices X and Y essentially represent sets of stress value vectors for each curve.

Sub-functional f_2 is the relative sum of local Frobenius norms, computed for each isochronous curve separately, after which the average norm value for the set of curves is calculated:

$$f_2 = \frac{1}{N_\tau} \sum_{j=1}^{N_\tau} \frac{\left|\left|\overline{y}_j - \overline{x}_j\right|\right|}{\left|\left|\overline{x}_j\right|\right|}, \tag{8}$$

where N_τ is the number of isochronous curves, $X = \sum_{j=1}^{N_\tau} \overline{x}_j$, $Y = \sum_{j=1}^{N_\tau} \overline{y}_j$.

Sub-functional f_3 is the maximum relative deviation between the approximated and approximating curves across the entire family of curves:

$$f_3 = \max\left(\max\left(\frac{\overline{y}_j - \overline{x}_j}{\overline{x}_j}\right)\right), \ j \in [1, N_\tau]. \tag{9}$$

Sub-functional f_4 is the relative Euclidean norm of the maximum relative deviations of each curve:

$$f_4 = \frac{1}{N_\tau} \sqrt{\sum_{j=1}^{N_\tau} err_j^2}, \ err_j = \max\left(\frac{\overline{y}_j - \overline{x}_j}{\overline{x}_j}\right), \tag{10}$$

where err_j is the relative deviation between the approximated and approximating curves.

Sub-functional f_5 is an integral criterion that evaluates the local relative deviation of the integrals of the two curves, which are then assessed using the relative Euclidean norm:

$$f_5 = \frac{1}{N_\tau}\sqrt{\sum_{j=1}^{N_\tau} int_j^2}\,,\ int_j = \frac{\left|\int_0^t \overline{y}dt - \int_0^t \overline{x}dt\right|}{\max\left(\int_0^t \overline{x}dt, \int_0^t \overline{y}dt\right)}, \quad (11)$$

where t is the calculation time.

The form of each sub-functional shows that their values range from 0 to 1, allowing for a combined functional comprising quantities of similar orders of magnitude. The procedure iteration concludes after a specified number of iterations is reached, upon which the parameter values yielding the minimal functional value are output. The sufficiency of iterations is checked by analyzing the convergence of the iterative process results.

After obtaining the optimal set of parameters, a numerical solution for the problem of uniaxial tension of a specimen is performed using the finite element method. A kinematic loading condition is applied, inducing a total strain of 2 % by the end of the calculation.

The material is considered viscoelastic: density, elastic modulus, Poisson's ratio, and the creep model parameters (according to the identification stage results) are specified. An arbitrary creep model can be implemented in Abaqus using the user subroutine CREEP [30]. For implementing simple creep models in metals, it is sufficient to define two quantities in this subroutine: the increment of creep strain over one integration time step and the derivative of the creep strain increment with respect to stress (the solution Jacobian). For the considered Norton-Bailey model, these relations are:

$$\Delta\varepsilon_{cr} = \varepsilon_0^{m+1}\left(\frac{\tilde{q}}{\sigma_0}\right)^n \cdot \left[\frac{1}{1+m}\left(t^{m+1} - (t-\Delta t)^{m+1}\right)\right], \frac{\partial \Delta\varepsilon_{cr}}{\partial \tilde{q}} = \Delta\varepsilon_{cr} \cdot (n/\tilde{q}\,). \quad (12)$$

The numerical simulation in Abaqus [30] employs an implicit time integration scheme for the equations of geometrically and physically nonlinear viscoelasticity within a quasi-static formulation (neglecting inertial forces).

Results and Discussion

The outcome of the identification procedure is an optimal set of parameters for the selected creep model. Table 1 presents the parameter values identified by the procedure for steel 12Kh18N12T/12Kh18N10T (AISI 321) at temperatures of 500, 550, and 600 °C. For convenience in further use of the parameters, all values are given in the SI system.

Table 1. Parameters of the Norton-Bailey model for steel 12Kh18N12T/12Kh18N10T (AISI 321)

T, °C	ε_0	σ_0, MPa	m	n
500	2.7013e-07	604.78	-0.7995	3.8593
550	2.4694e-09	338.76	-0.7076	4.3129
600	1.0412e-08	344.63	-0.6607	3.6015

The convergence of the procedure and the optimal functional value are demonstrated in Fig. 2 for each temperature and its corresponding parameter set. The number of iterations of the procedure is plotted on the abscissa axis, and the value of the inverse functional, which is being minimized, is plotted on the ordinate axis. The inverse value is used because initial perturbing values that inflate the functional value arise during the procedure, complicating the visualization of results.

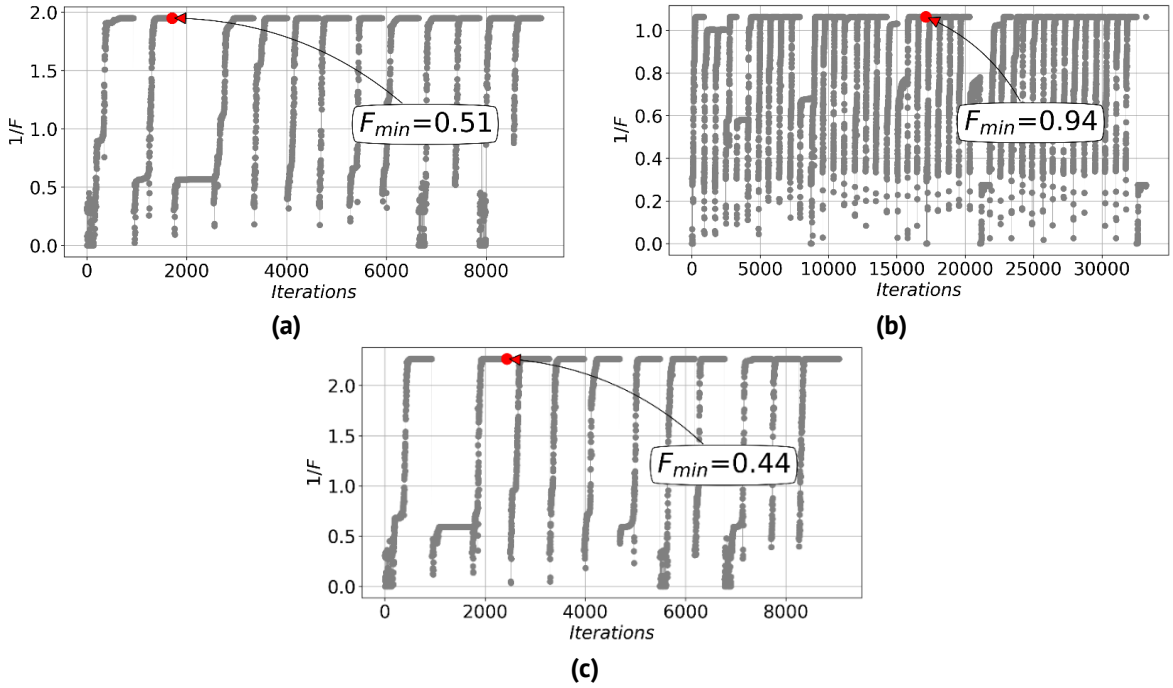

Fig. 2. Identification procedure results at (a) 500 °C, (b) 550 °C, and (c) 600 °C

Each "vertical" set of points represents one iteration of the optimization procedure. It is evident that in each iteration, the procedure finds a final parameter value close to the optimal one, indicating its stability and convergence (no need for additional refinement iterations). Moreover, this optimal value is achieved within the first few iterations of the procedure.

The identified parameters are assigned to the user-defined creep model in Abaqus, after which the calculation of uniaxial tension of a viscoelastic specimen is performed. The simulation results for different loading rates yield material stress-strain diagrams, which are subsequently compared with the standard isochronous curves. Figures 3–5 demonstrate the standard and numerical curves.

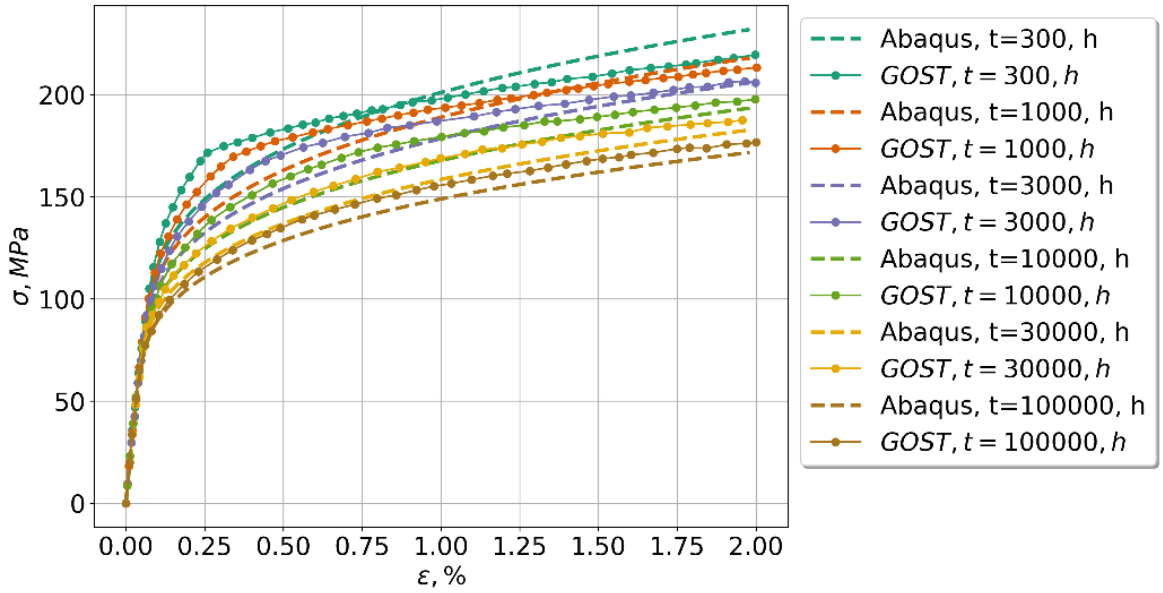

Fig. 3. Isochronous curves for AISI321 steel, T = 500 °C

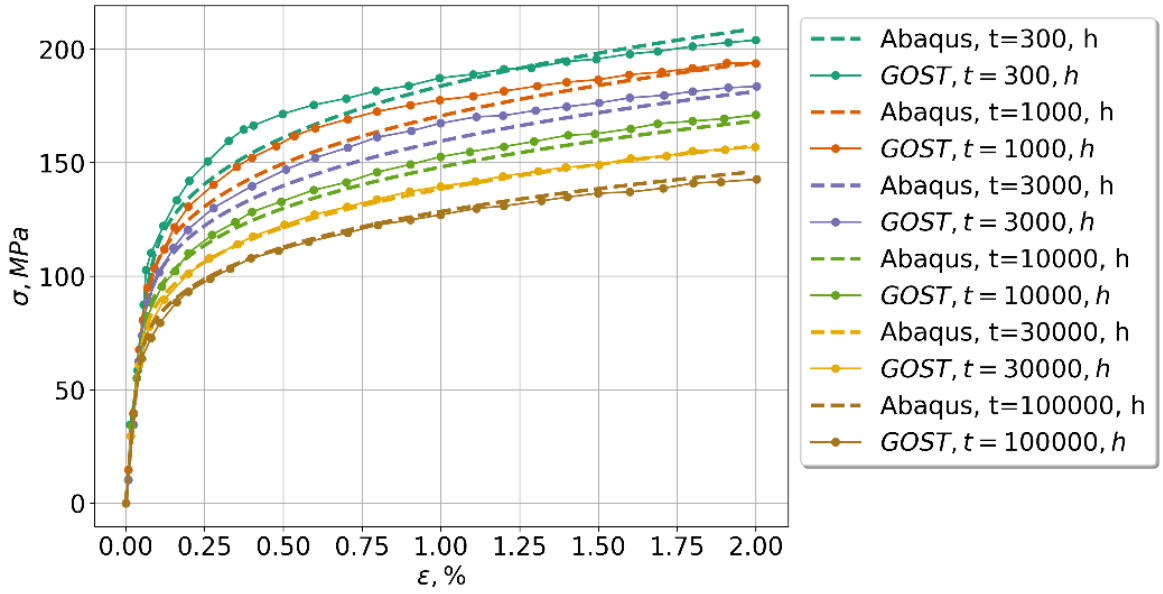

Fig.4. Isochronous curves for AISI321 steel, T = 550 °C

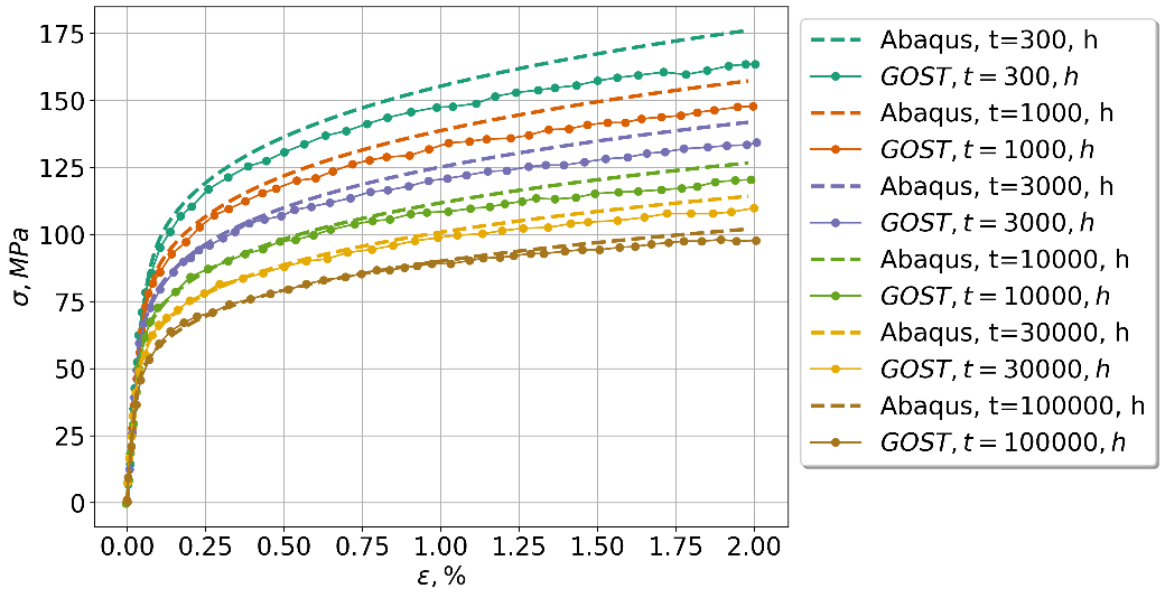

Fig. 5. Isochronous curves for AISI321 steel, T = 600 °C

Good agreement between the curves is observed for all temperatures at times exceeding 10,000 h. For shorter times, a larger discrepancy in the results is noted. For a quantitative assessment of the adequacy of the identified parameters, an analysis of the maximum and average deviation of the curves at different times for the three temperatures was performed (Fig. 6). The time corresponding to the isochronous curve required to reach 2 % strain, normalized to the maximum time value among the entire set of curves, is plotted on the abscissa axis. The quantities are determined pointwise, forming an array of local deviations, after which the maximum and average error values for the entire curve are determined:

$$err_{max} = \max\left(\left|\frac{\sigma_{norm}-\sigma_{abq}}{\sigma_{norm}}\right|\right),\ err_{mean} = \overline{\left|\frac{\sigma_{norm}-\sigma_{abq}}{\sigma_{norm}}\right|}, \quad (13)$$

where err_{max} and err_{mean} are the maximum and average errors, respectively, σ_{norm} and σ_{abq} are the stresses according to the standard and numerical (Abaqus) isochronous curves, respectively.

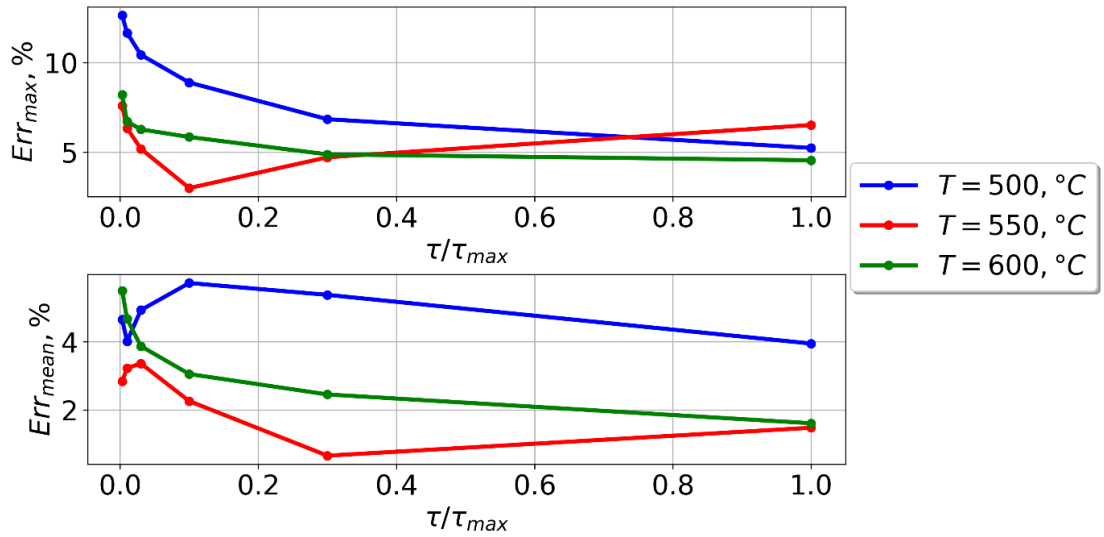

Fig. 6. Maximum and average deviations between standard and numerical curves for all analyzed cases

The maximum deviation between the curves does not exceed 13 %, and it is observed for fast loading rates. For slow loading rates, a decrease in both the maximum and average error is observed. The average error for all analysed cases does not exceed 5 %.

Discrepancies in results at short loading durations are associated with the limitations of the Norton-Bailey model. Its modification can be implemented, for example, by considering approaches mentioned in [27]0 or by introducing a separate set of creep model parameters for times less than 3000 h. Table 2 presents the model parameters for such short-term exposure. Figures 7–9 show normative and numerical isochronous curves obtained using the identified parameters.

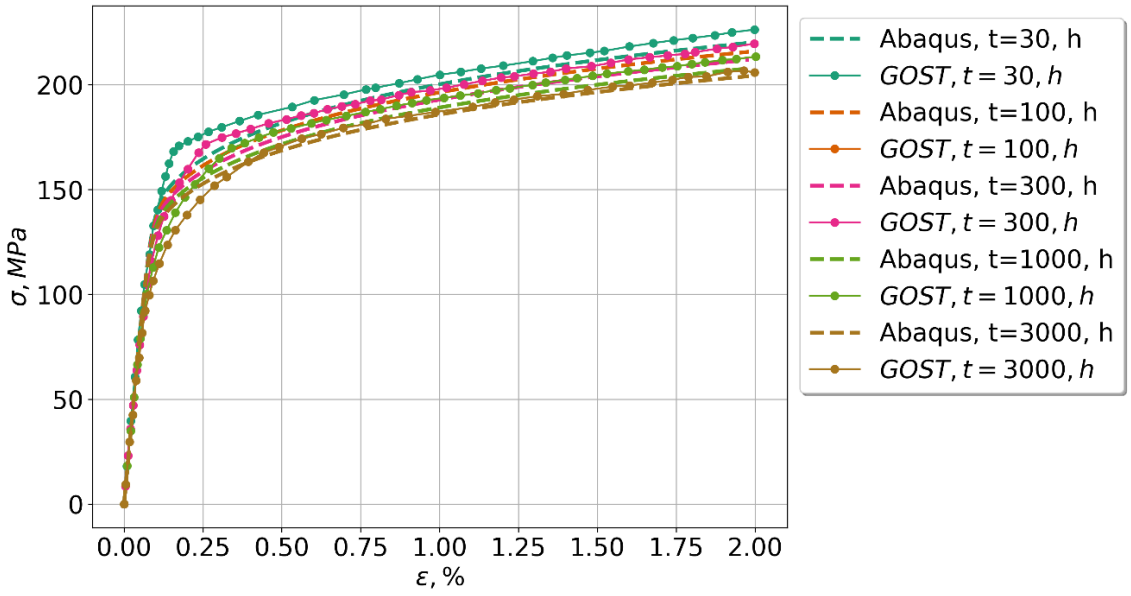

Fig. 7. Isochronous curves for AISI321 steel for $t < 3000$ h, $T = 500$ °C

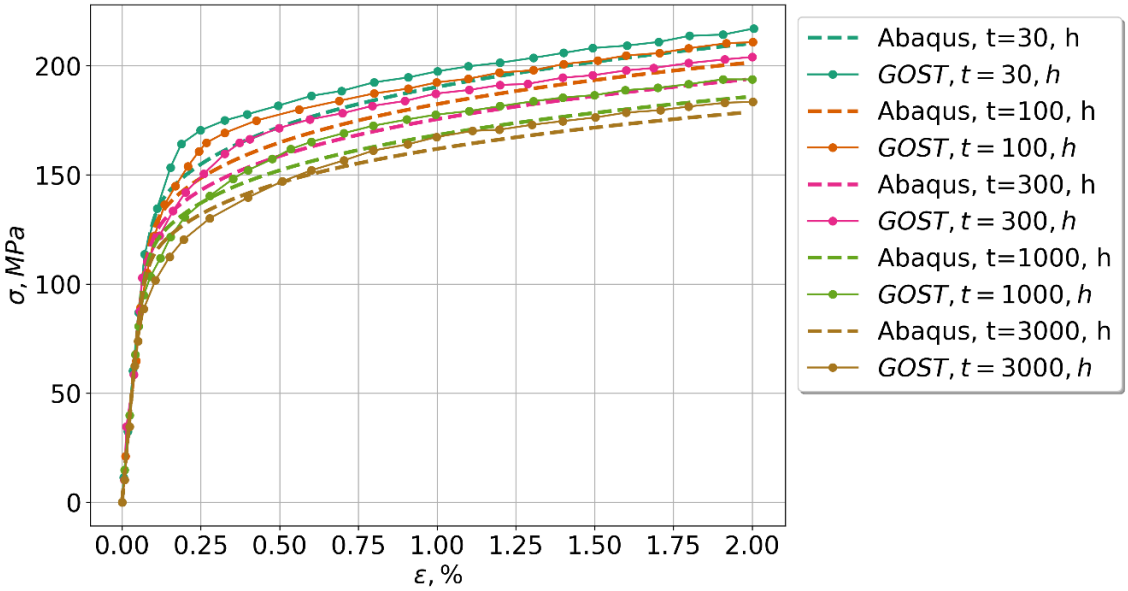

Fig. 8. Isochronous curves for AISI321 steel for $t < 3000$ h, $T = 550$ °C

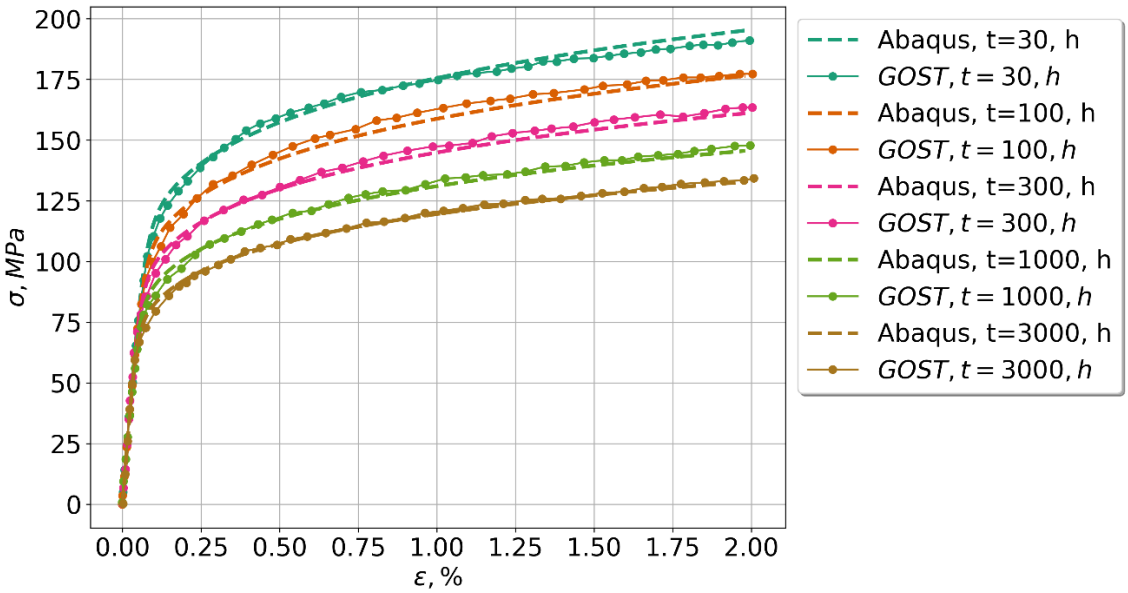

Fig. 9. Isochronous curves for AISI321 steel for $t < 3000$ h, $T = 600$ °C

Table 2. Parameters of the Norton-Bailey model for steel 12Kh18N12T/12Kh18N10T (AISI 321) for $t < 3000$ h

T, °C	ε_0	σ_0, MPa	m	n
500	2.4856e-09	352.28	-0.8937	6.5109
550	1.6635e-08	340.11	-0.8034	5.5911
600	3.5435e-08	313.22	-0.6487	4.1957

Conclusions

This paper presents the results of developing an automated procedure for identifying the parameters of an arbitrary creep model, demonstrated using the Norton-Bailey model based on a set of isochronous curves at a constant temperature. The results are presented for steel grade 12Kh18N12T/12Kh18N10T (AISI 321) at temperatures of 500, 550, and 600 °C.

Good agreement is demonstrated between the standard creep curves and the numerical curves obtained in Abaqus using the developed model with the identified parameters. The maximum deviation between the calculated and standard curves does not exceed 13 % for fast loading rates and 8 % for slow loading rates. On average, the deviation between the curves does not exceed 5 % for all analyzed cases and decreases with slower loading rates.

CRediT authorship contribution statement

Roman V. Fedorenko: investigation, conceptualization, writing – original draft; **Aleksei V. Lukin**: supervision, writing – review & editing.

Conflict of interest

The authors declare that they have no conflict of interest.

References

1. *Decree of the President of the Russian Federation No. 529, dated 18 June 2024. On the Approval of the Priority Areas for Scientific and Technological Development and the List of Critical Science-Intensive Technologies*. Available from: http://www.kremlin.ru/acts/bank/50755 [Accessed 17th February 2026]. (In Russian)
2. Adamov EO, Kaplienko AV, Orlov VV, Smirnov VS, Lopatkin AV, Lemekov VV, Moiseev AV. Fast neutron reactor with lead coolant BREST: from concept to technology implementation. *Atomic Energy*. 2020;129(4): 185–194. (In Russian)
3. Shamarin IV, Gavrilov PM. High-temperature nuclear power technologies. *Izvestiya Tomskogo Politekhnicheskogo Universiteta*. 2010;316(4): 5–9. (In Russian)
4. Krasilnikov AV, Konovalov SV, Bondarchuk EN, Masul IV, Rodin IY, Mineyev AB, Kuzmin EG, Kavin AA, Karpov DA, Leonov VM, Hayrutdinov RR, Kukushkin AS, Pornov DV, Ivanov AA, Belchenko YI, Denisov GG. Tokamak with reactor technologies (TRT): concept, missions, main features and expected characteristics. *Plasma Physics*. 2021;47(11): 970–985. (In Russian)
5. Rabotnov YV. *Creep of structural elements*. Moscow: Nauka; 1966. (In Russian)
6. Le X, Takaki K, Takamoto I. Creep-fatigue life evaluation of type 304 stainless steel under non-proportional loading. *International Journal of Pressure Vessels and Piping*. 2021;194: 104467.
7. Lokoshchenko AM. *Creep and long-term strength of metals*. Moscow: Fizmatlit; 2016. (In Russian)
8. Lokoshchenko AM, Teraud VV. Creep of a long narrow membrane under constrained conditions until failure. *Journal of Applied Mechanics and Technical Physics*. 2013;54(3): 126–133 (In Russian)
9. National Standard of the Russian Federation. GOST R 59115.10-2021. *Rules for strength assessment of equipment and pipelines of nuclear power installations. Confirmatory analysis on stage of design*. Moscow: Standartinform; 2021. (In Russian)
10. American Society of Mechanical Engineers. ASME BPVC.III.5-2015. *Division 5 – High Temperature Reactors*. New York: ASME; 2015.
11. Norton FH. *The Creep of Steels at High Temperatures*. New York: McGraw-Hill; 1929.
12. Betten J. *Creep Mechanics*. 2nd ed. Berlin: Springer; 2005.
13. May D, Gordon A, Segletes D. The Application of the Norton-Bailey Law for Creep Prediction Through Power Law Regression. In: *Proceedings of the ASME Turbo Expo*. 2013. p.GT2013-96008.
14. Darveaux R, Banerji K. Constitutive relations for Tin-based Solder Joints. *IEEE Transactions on Components, Hybrids, and Manufacturing Technology*. 1992;15(6): 1013–1024.
15. Kachanov LM. On the time to failure under creep conditions. *Izvestiya Akademii Nauk SSSR, Otdelenie Tekhnicheskikh Nauk*. 1958;(8): 26–31. (In Russian)
16. Rabotnov YN. On the mechanism of long-term fracture. In: *Problems of strength of materials and structures*. Moscow: USSR Academy of Sciences Publishing House; 1959. p.5–7. (In Russian)
17. Rabotnov YN. On creep rupture. *Journal of Applied Mechanics and Technical Physics*. 1963;(2): 113–123. (In Russian)

18. Hong J, Wang T, Zhu B, Li D, Dong H, Zuo D, Huang J, Man Z, Zhang G. Enhancing creep life prediction under large-shear deformation based on a modified Kachanov–Rabotnov model. *Nuclear Engineering and Design*. 2026;448: 114694.
19. Kachanov LM. *Fundamentals of fracture mechanics*. Moscow: Nauka; 1974. (In Russian)
20. Sandström R. Tertiary Creep. In: *Basic Modeling and Theory of Creep of Metallic Materials*. Cham: Springer; 2024. p.233–256.
21. Saitova RR, Arutyunyan AR. Creep and long-term strength of high-entropy alloys. *Materials Physics and Mechanics*. 2025;53(3): 116–121.
22. Othman AM, Hayhurst DR, Dyson BF. Skeletal point stresses in circumferentially notched tension bars undergoing tertiary creep modelled with physically based constitutive equations. *Proceedings of the Royal Society of London. Series A, Mathematical and Physical Sciences*. 1993;441(1912): 343–358.
23. National Standard of the Russian Federation. GOST R 59115.4-2021. *Rules for strength assessment of equipment and pipelines of nuclear power installations. Long-term mechanical properties of structural materials*. Moscow: Standartinform; 2021. (In Russian)
24. Grishchenko AI, Semenov AS. Effective methods of parameter identification for creep models with account of III stage. *MATEC Web of Conferences*. 2016;53: 01041.
25. Grishchenko AI, Semenov AS, Getsov LB. Modeling inelastic deformation of single crystal superalloys with account of γ/γ' phases evolution. *Material Physics and Mechanics*. 2015;24(4): 325–330.
26. Shirmer RW, Selent M, Abendroth M, Kiefer B. Identification of creep parameters from multi-step relaxation tests on miniaturised specimen. *Proceedings in Applied Mathematics and Mechanics*. 2023;23(4): e202200144.
27. Liu Y, Murakami S. Damage localization of conventional creep damage models and proposition of a new model for creep damage analysis. *JSME International Journal, Series A: Solid Mechanics and Material Engineering*. 1998;41(1): 57–65.
28. Katanakha NA, Semenov AS, Getsov LB. Unified model of steady-state and transient creep and identification of its parameters. *Strength of Materials*. 2013;45(4): 495–505.
29. Tashakori S, San-Millan A, Vaziri V, Aphale SS. Fast Parameter Identification of the Fractional-Order Creep Model. *Actuators*. 2024;13(12): 534.
30. *Abaqus 2017 Theory Guide*. Providence, RI: Dassault Systèmes; 2017.
31. Endres SC, Sandrock C, Focke WW. A simplicial homology algorithm for lipschitz optimization. *Journal of Global Optimization*. 2018;72(1): 181–217.
32. Conn AR, Scheinberg K, Vicente LN. *Introduction to Derivative-Free Optimization*. Philadelphia: Society for Industrial and Applied Mathematics; 2009
33. Kelley CT. *Iterative Methods for Optimization*. Philadelphia: Society for Industrial and Applied Mathematics (SIAM); 1999
34. Gantmakher FR. *Theory of matrices*. 5th ed. Moscow: Fizmatlit; 2004. (In Russian)